The 4th International Online Conference on Nanomaterials

Investigation of Transition Metal ion Cu^{2+} and Mg^{2+} doped zinc aluminate ($ZnAl_2o_4$) and their structural, spectral, optical, and dielectric study for high frequency applications.

.

Yasmin J , Gracie P J and Geetha D*

Department of Applied Sciences and Humanities, Madras Institute of Technology, Anna University, Chennai-44, India

5-19 May 2023

OUTLINE

- INTRODUCTION
- OBJECTIVES
- METHODS
- RESULTS
- CONCLUSION

INTRODUCTION

- Zinc Aluminate is an excellent dielectric material suitable for microwave applications by virtue of their high-quality factor, low loss and better conductivity.
- In normal spinel structure given by the formula $(Zn)^{tet}(Al)_2{}^{oct}O_4$, the vacant 56 tetrahedral and 16 octahedral sites and the order-disorder transitions of cations at these sites open the window of possibility to design these properties by doping.
- The influence of doping of Cu^{2+} and Mg^{2+} at A site has been investigated and it has been found to be highly electrical resistive with low dielectric constant and very small dielectric loss which are highly required for applications like electrical insulation, capacitors, substrates for integrated circuits, and microwave technology.
- In this regard, the replacement of Cu and Mg site in $ZnAl_2O_4$ could modify the band gap of resultant material widening its range of applications

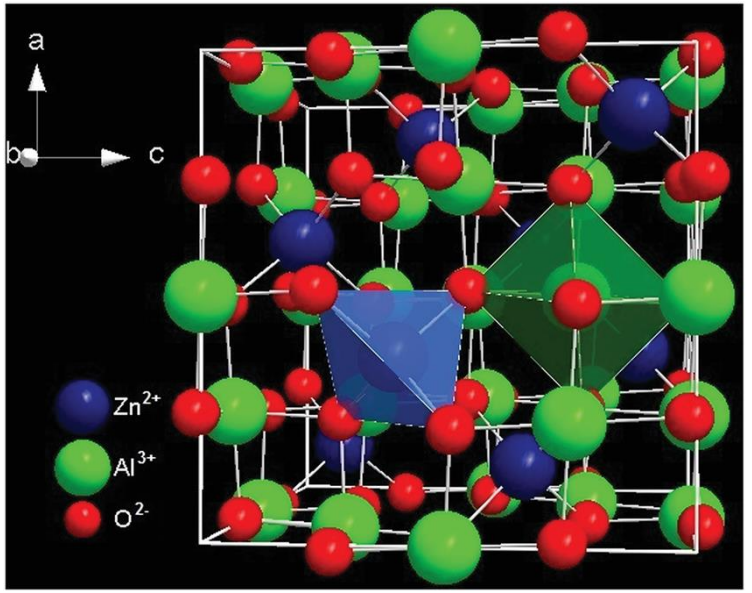

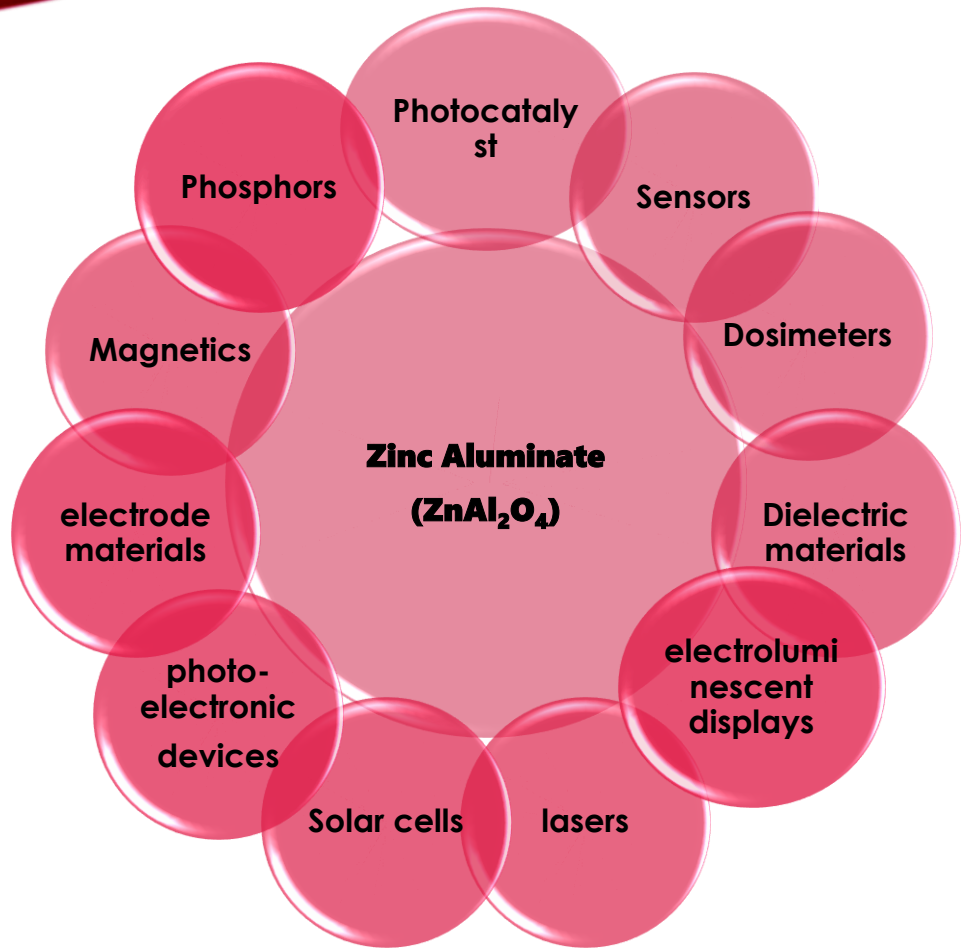

Zinc Aluminate $(ZnAl_2O_4)$

- high mechanical resistance
- large surface area
- good cationic dispersion
- low stability
- high strength
- high melting temperature
- high thermal and chemical stability
- hydrophobicity
- low electrical permittivity
- non toxicity
- wide band gap

OBJECTIVES

- To synthesize of Cu^{2+} and Mg^{2+} doped Zinc Aluminate through sol-gel method.
- To investigate the effect Cu^{2+} and Mg^{2+} ions on structural and dielectric behavior of $ZnAl_2O_4$ with general formula $Zn_{1-x}M_xAl_2O_4$ where $M=Cu^{2+}$, Mg^{2+}($x = 0, 0.10$).
- To analyze the potential of the prepared aluminates that can be used for optoelectronic applications, low-frequency devices, and also to test its utility that might be used as a potential candidate in magnetic and catalysis applications.

METHODS

- Numerous wet chemical and solid-state methods for the synthesis of $ZnAl_2O_4$ nanocrystalline particles have been reported, including solution combustion, hydrothermal, sol gel, co precipitation, solid phase, rapid thermal annealing, microwave solution route, solvothermal and others.
- Among all, the Solution Combustion Synthesis (SCS) is a one-of-a-kind method for the preparation of ZA particles in its as-prepared form.
- Other advantages include the ability to produce fine particles having large surface area in its as-synthesis form at relative low temperature.
- This is a vacuum-free technique which employs basic equipment to control the purity, homogeneity, and stoichiometry with amount of doping.

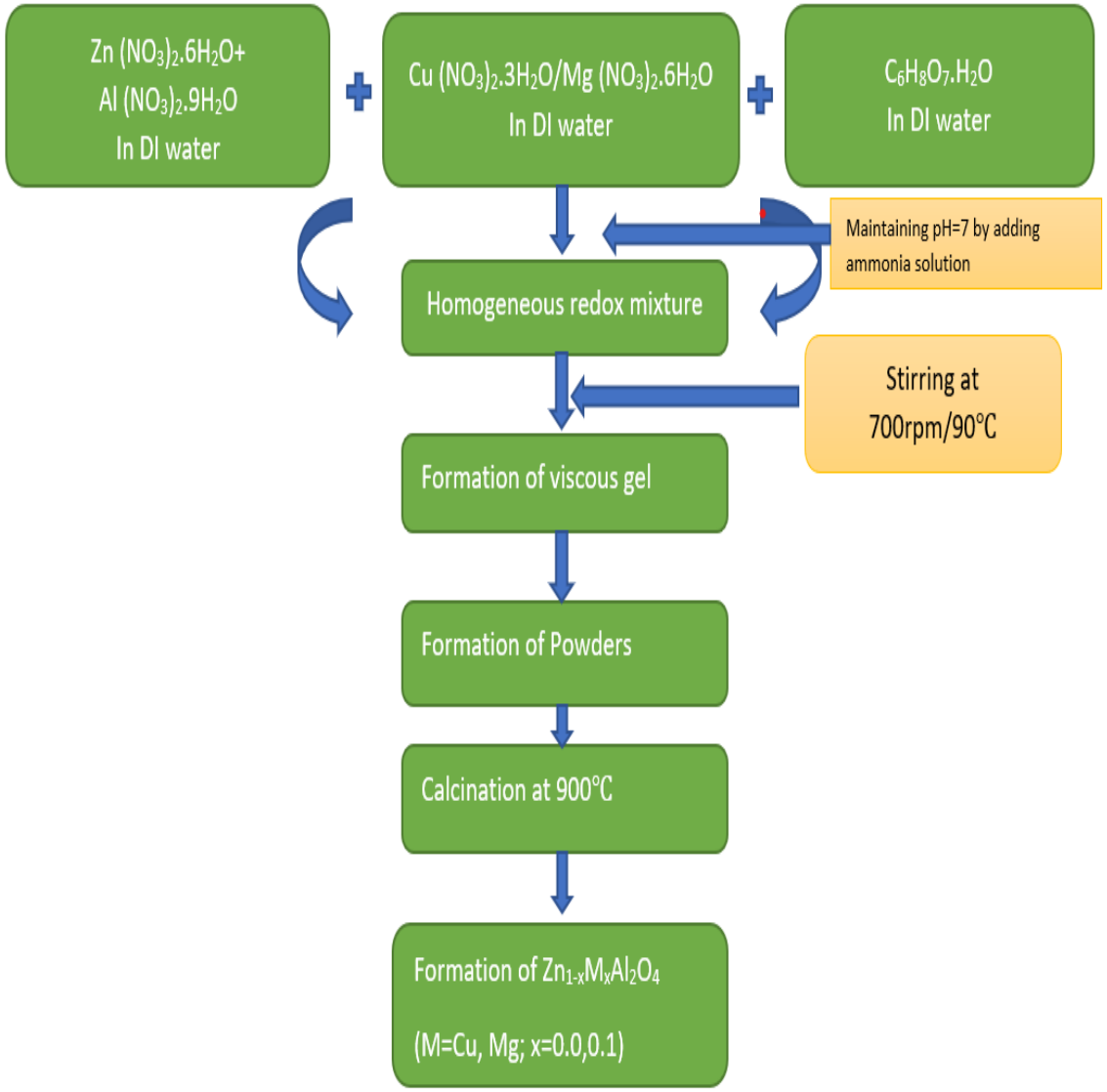

RESULTS AND DISCUSSIONS

- Structural analysis-XRD
- Functional group analysis-FTIR
- Band gap analysis-UV-DRS
- Dielectric Measurements-Impedance Analyser
- Composition analysis-EDAX

STRUCTURAL ANALYSIS-XRD

- The investigation of crystalline phases and phase purity present in the prepared aluminates was measured by x-ray diffraction (XRD) technique.
- Fig. 1 depicts the XRD pattern of $ZnAl_2O_4$ (ZA), $Zn_{0.9}Cu_{0.1}Al_2O_4$ (ZAC) and $Zn_{0.9}Mg_{0.1}Al_2O_4$ (ZAM) prepared by the sol–gel combustion method. The obtained pattern coincided with the $ZnAl_2O_4$ cubic spinel crystal structure and indexed with the miller indices (111), (2 2 0), (3 1 1), (4 0 0), (331), (422), (511), (440), (620) and (533) corresponding to the various planes.
- The diffracted peaks of $ZnAl_2O_4$ were found well-matched with JCPDS Card No. 05–0669 and the previous reported literatures.
- The crystallite size is calculated by the highly intensive full width half maximum diffraction peak of the prepared materials using Scherer's equation,

$$D_{XRD} = \frac{k\lambda}{\beta\cos\theta}$$

The average crystallite size increases for Cu and Mg doped sample and it was calculated to be in the range 21-23nm.

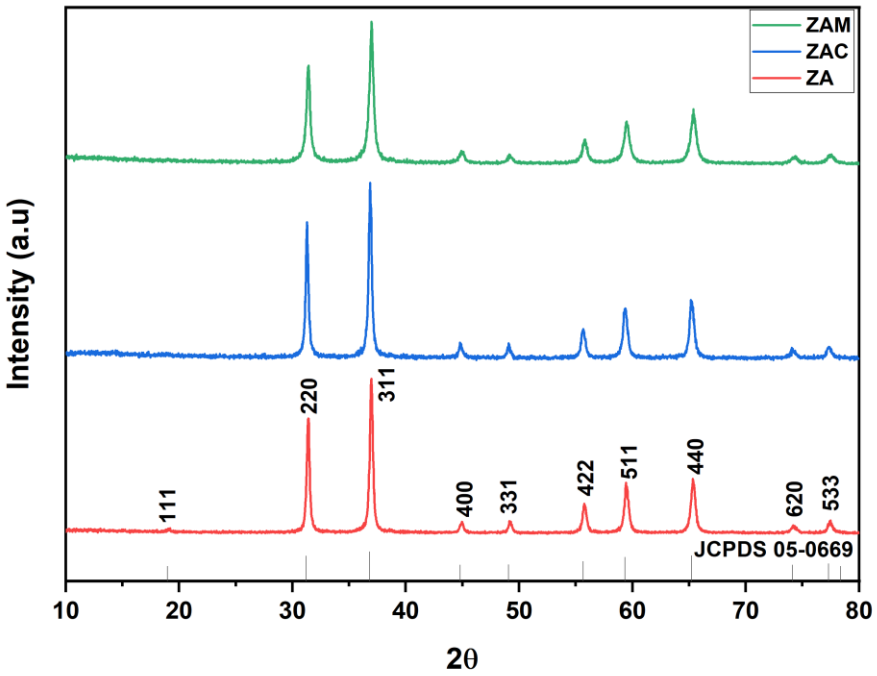

Figure 1. XRD Diffractogram of (ZA), (ZAC) and (ZAM)

FUNCTIONAL GROUP ANALYSIS-FTIR

- Fig. 2 depicts the FTIR spectra of $ZnAl_2O_4$ (ZA), $Zn_{0.9}Cu_{0.1}Al_2O_4$ (ZAC) and $Zn_{0.9}Mg_{0.1}Al_2O_4$ (ZAM) prepared by the sol–gel combustion method. The presence of absorption bands at 661.53, 554.49, 496.63 cm^{-1} corresponds to the vibration of Zn-O, Al-O and Zn-O-Al at tetrahedral and octahedral sites respectively.
- The sharpness of the bands defines the porous nature of the synthesized samples. The presence of bands at 2354.27cm^{-1} is due to CO_2 absorbed from air. The broad bands at 3437.8 corresponds to -OH stretching absorbed on the surface of the water molecule.
- The bands at 1627 and 1408cm^{-1} are attributed to the symmetric and asymmetric vibrations of C-H.

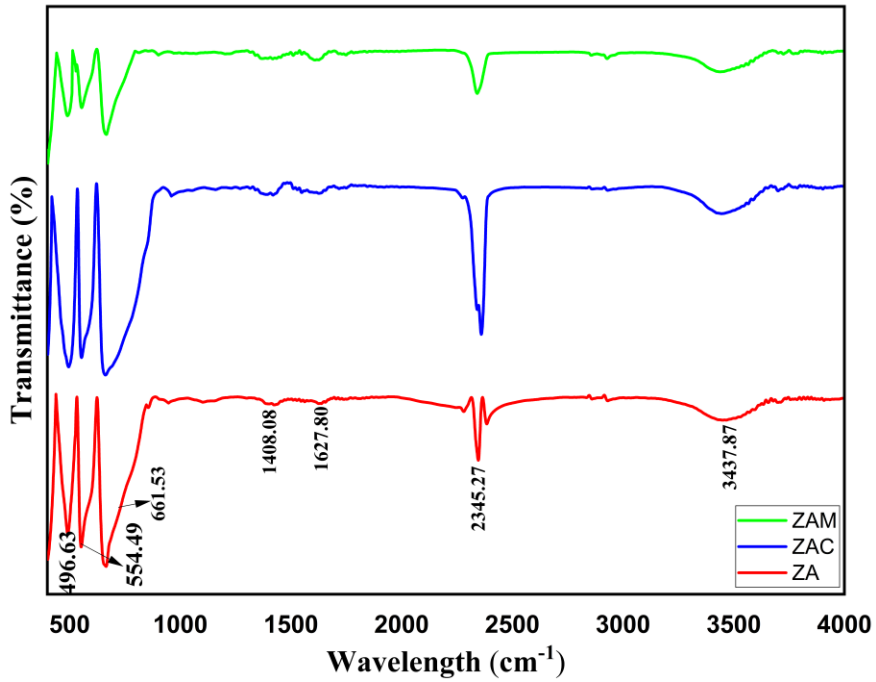

Figure 2. FTIR spectra of (ZA), (ZAC) and (ZAM)

COMPOSITIONAL ANALYSIS-EDAX

- Figure 3 a,b,c shows the energy dispersive X-ray (EDX) spectrum of Zinc aluminate samples indicating the existence of O, Zn, Cu, Mg and Al elements in the ZA, ZAC and ZAM compounds.
- The percentages of each element of ZA, ZAC and ZAM are obtained from energy dispersive X-ray spectrum.

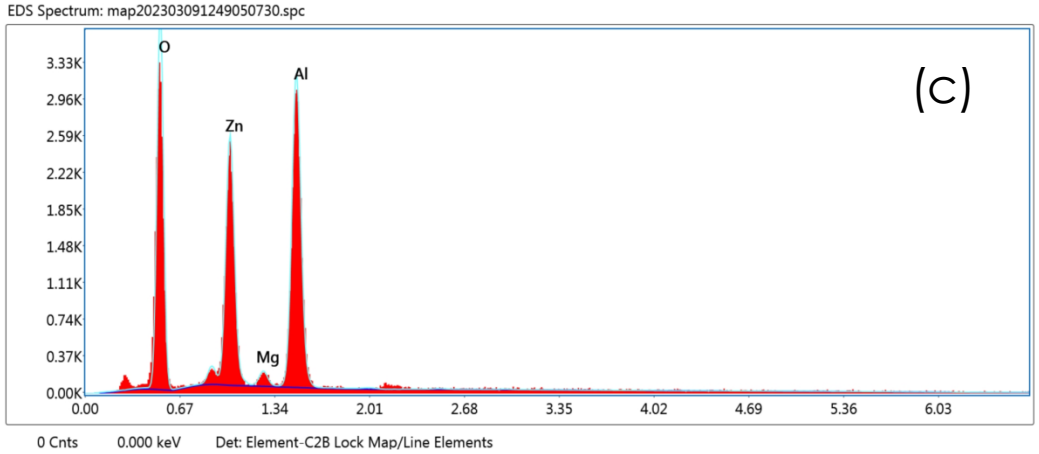

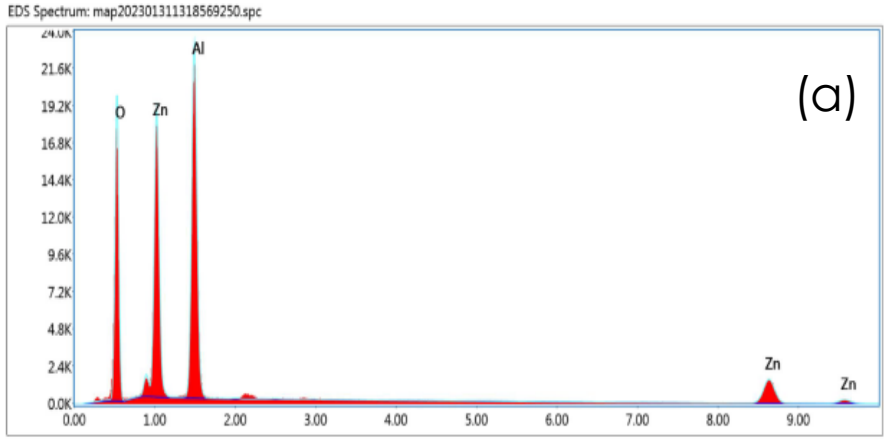

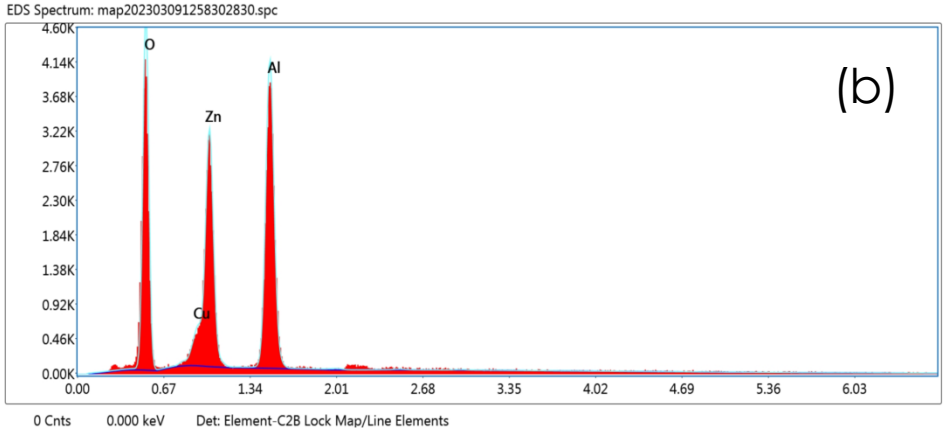

Figure 3: EDX Spectrum Of (a)ZA (b) ZAC and (c) ZAM Samples

BAND GAP ANALYSIS-UV DRS

- The absorption spectra of ZA, ZAC and ZAM particles in DRS mode were recorded in the wavelength range of 200– 800 nm. For a direct bandgap semiconducting material, the absorption coefficient near the band edge is given by

$$\alpha = \frac{A}{h\vartheta}(h\vartheta - E_g)^{1/2}$$

- The optical band gap is determined by plotting $(\alpha h\nu)^2$ against $h\nu$ and finding the intercept on the $h\nu$ axis by extrapolating the plot to $(\alpha h\nu)^2 = 0$ as shown in Fig4. From the Kubelka Munk's plot the values of band gap is calculated to be 3.03eV(ZA), 2.94eV(ZAC) and 2.90eV(ZAM).

- We found that the optical band gap value decreases, which refer to the redshift and can be attributed to the quantum confinement effect due to small size of Zinc Aluminate particles.

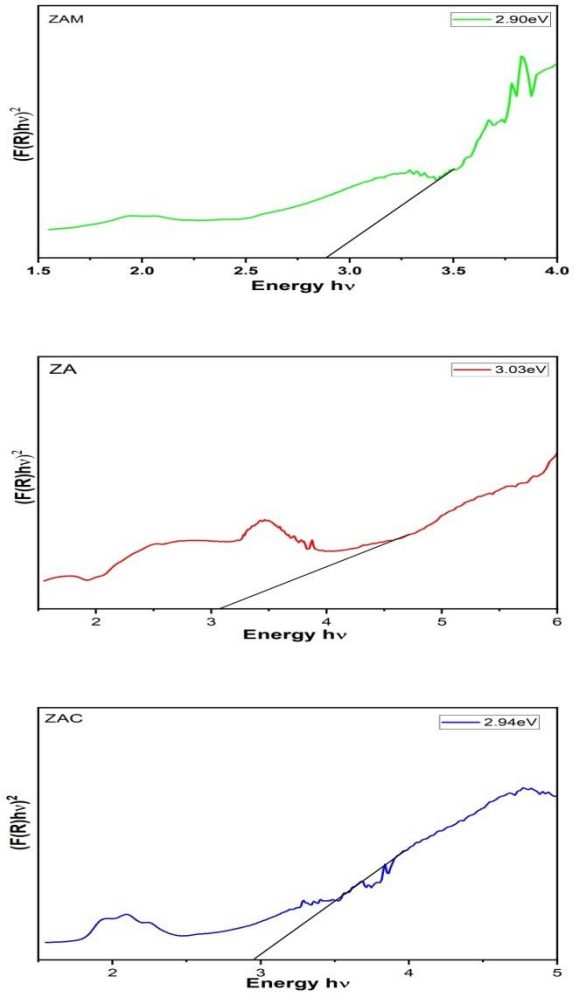

Figure 4. Tauc's plot of ZA, ZAC and ZAM

DIELECTRIC MEASUREMENTS-DIELECTRIC CONSTANT

- From Figure 5, we found that at the low-frequency region, the magnitude of the real part of dielectric constant is high which may due be Maxwell–Wagner (M–W) space charge polarization due to electrode sample interfacial effect.
- Thereafter, the real part of dielectric constant decreases with the increase of frequency due to the fact that the polarization decreases with increasing frequency and then reaches a constant value at the high-frequency limit.
- Also, from Figure 5, it is quite clear that the value of dielectric constant decreases after the replacement of Cu^{2+} and Mg^{2+} for the in place of Zn due to the mismatch in the occupation of the site starts decreasing leading to the decrease in density and hence the volume increases and as a result, it starts responding to the applied field.

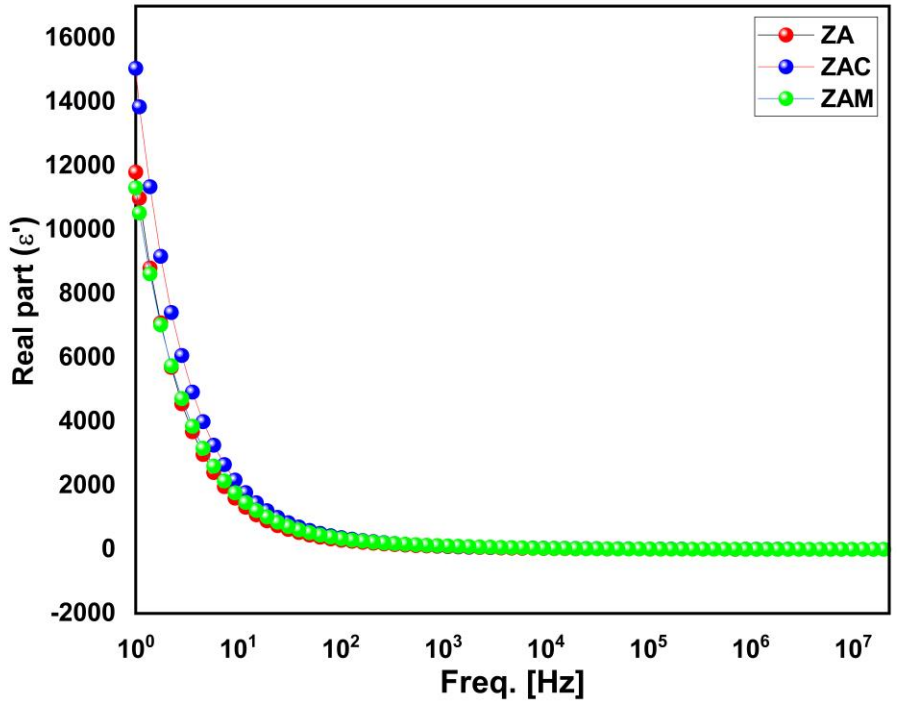

Figure 5: Frequency dependent dielectric constant ($\boldsymbol{\varepsilon'}$)of (ZA), (ZAC) and (ZAM)

DIELECTRIC TANGENT LOSS

- The dielectric loss tangent (tan δ) of zinc aluminate samples measured at room temperature is shown in Figure.6.
- In the mid-frequency region, the relaxation peaks were observed along with the decrement in the loss tangent in lower and higher frequency regions. For ZAM sample, the high magnitude of relaxation peak at the low-frequency region may be due to space charge polarization or due to grain boundary polarization, for exchange interactions at the Al site (i.e., octahedral co-ordinate).
- The decrease in dielectric loss tangent with increase in frequency is in accordance with the Koop's phenomenological model
- The conduction mechanism in spinel aluminate is considered to involve the hopping of electrons via the interaction between the exchange ions of Al^{3+} and Al^{2+} at the octahedral site.

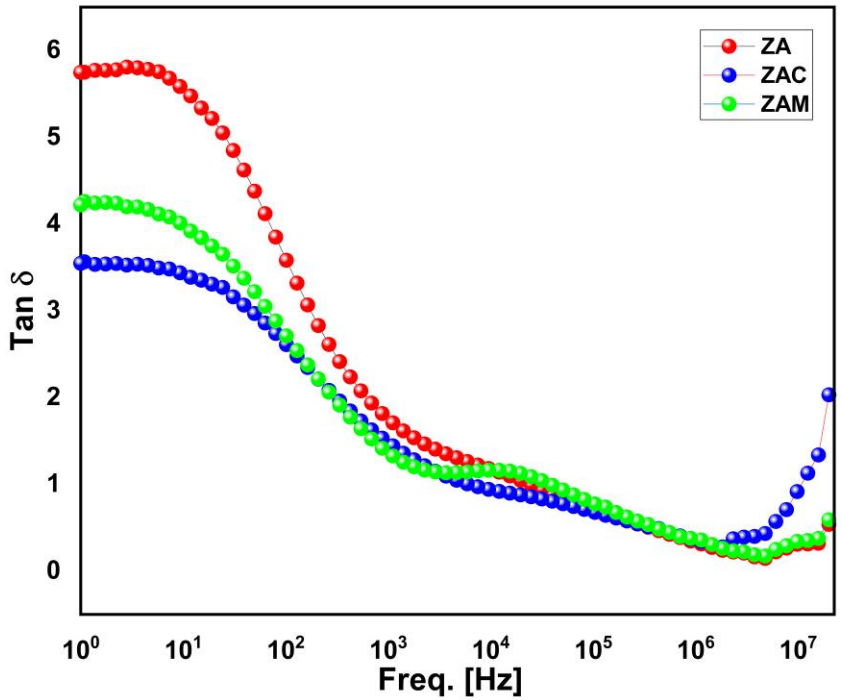

Figure 6: Frequency dependent dielectric loss tangent (tan δ) of (ZA), (ZAC) and (ZAM)

COLE-COLE PLOT

- Cole-Cole plot helps to understand the electrical properties of materials with variation of inter grain, intra grain and electrode effects. The relaxation mechanisms involved is closely related to the shape of the curve and the number of semicircles obtained.
- The figure shows the measured Cole–Cole plots of under different frequencies which exhibits one semicircle(grains) and an arc of circle (grain boundaries).
- The inclined straight line attached to the semicircle indicates the partial blocking of the charge carriers at the boundary regions which ultimately results in the decrease in electronic conductivity which is also attributed to the decrease in diameter of the circle for ZAC and ZAM.

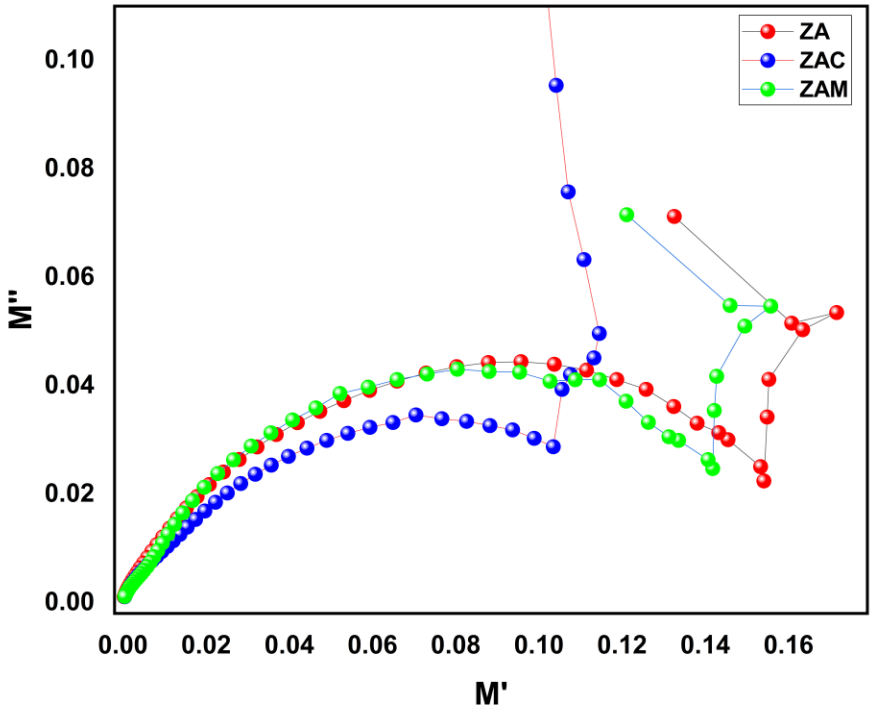

Figure 7: Cole-Cole Plot Of ZA, ZAC and ZAM Samples

CONCLUSIONS

- The XRD of aluminates displayed their single-phase spinel structure and it was found the replacement of Cu and Mg ions content decreases the lattice parameter (8.09-8.05nm) and an increase in crystallite size(21-23nm) was observed when compared to the parent sample.
- The absorption band in the range 554 cm^{-1} for the octahedral O_h site and 661cm^{-1} for the tetrahedral T_d site of aluminates was confirmed by FTIR spectra. The presence of elements in the ZA, ZAC and ZAM samples were confirmed by EDAX spectrum.
- From the optical band gap measurements which was calculated using Kubelka-Munk function, it was observed that with the substitution of Cu and Mg in the mother sample a gradual decrease in band gap value (3.03-2.90eV) was observed, indicating a redshift in zinc aluminate samples.
- The frequency dependence of real and imaginary parts of the dielectric constant ε', Cole Cole plot and tangent loss (Tan δ) was analyzed at room temperature for all the samples and the observed results are reported. We observed the fall in dielectric permittivity and dielectric loss with the rise in the operating frequency.
- From the Cole Cole plot it was found that both grains and grain boundaries both contributed in the conduction process.
- The temperature dependent dielectric and impedance behavior will be investigated in the future studies.

REFERENCES

1.Akika FZ, Benamira M, Lahmar H, Trari M, Avramova I, Suzer. Structural and optical properties of Cu-doped ZnAl2O4 and its application as photocatalyst for Cr(VI) reduction under sunlight. Surfaces and Interfaces 2020; 18.

2.Varghese AA, Kuriakose E, Jose J, Aryal S, Khanal R, Anila EI. Investigations on the electronic properties and effect of chitosan capping on the structural and optical properties of zinc aluminate quantum dots. Appl Surf Sci 2022; 579.

3.Nirmala TS, Iyandurai N, Yuvaraj S, Sundararajan M. Third order nonlinear optical behavior and optical limiting properties of Ni2+ ions doped zinc nano-aluminates. Opt Mater (Amst) 2022; 124.

4.New fuel governed combustion synthesis and improved luminescence in nanocrystalline Cr3+ doped ZnAl2O4 particles. Results in Optics 2022; 8.

5.Navgare DL, Kawade VB, Shaikh SF *et al*. Structure-sensitive magnetic properties of nanocrystalline Co2+-substituted Ni–Zn ferrite aluminates. Ceram Int 2021; 47: 26492–26500.

6.Chen PC, Ganguly A, Kanna Sharma TS, Chou KY, Chang SM, Hwa KY. Investigation of T site variation in spinel aluminates TAl2O4 (T= Mg, Zn & Cu), and formation of electrocatalyst CuAl2O4/carbon for efficient sensing application. Chemosphere 2022; 301.

7.Elakkiya V, Agarwal Y, Sumathi S. Photocatalytic activity of divalent ion (copper, zinc and magnesium) doped NiAl2O4. Solid State Sci 2018; 82: 92–98.

8.Saleem M, Varshney D. Influence of transition metal Cr2+ doping on structural, electrical and optical properties of Mg-Zn aluminates. J Alloys Compd 2017; 708: 397–403.

9.Arifuzzaman M, Hossen MB, Afroze JD, Abden MJ. Structural and electrical properties of Cu substituted Ni–Cd nanoferrites for microwave applications. Physica B Condens Matter 2020; 588.

ACKNOWLEDGEMENTS

- I express my sincere thanks to my respected supervisor **Dr. D. GEETHA**, Assistant professor, Division of Applied Science and Humanities, Anna University (MIT Campus), Chennai for her guidance, expertise, kindness, and support from the very early stage of this work. Her directions and valuable comments helped me to fulfil the work and to move forward with investigation in depth.
- My sincere thanks and gratitude to **Dr. V. Ponnusamy**, Professor and Head of the department of Applied Sciences and Humanities, for offering me a great opportunity.
- I thank Anna University for providing me **Anna Centenary Research Fellowship ACRF** to carry out my research work easily.
- I thank **Sophisticated Instrumentation Facilities SCIF** of SRM University, Kattangulathur and Pondicherry University, Pondicherry for providing me the research facilities.
- Finally I thank my research colleague, my friends and my family members for their constant support.


Thank You